SIGNAL RECOVERY IN PERTURBED FOURIER COMPRESSED SENSING

Himanshu Pandotra[1]*, Eeshan Malhotra*[2]*, Ajit Rajwade*[2] *and Karthik S. Gurumoorthy*[3]

[1]Department of Electrical Engineering, Indian Institute of Technology Bombay
[2]Department of Computer Science and Engineering, Indian Institute of Technology Bombay
[3] International Center for Theoretical Sciences, Bengaluru

ABSTRACT

In many applications in compressed sensing, the measurement matrix is a Fourier matrix, *i.e.*, it measures the Fourier transform of the underlying signal at some specified 'base' frequencies $\{u_i\}_{i=1}^M$, where M is the number of measurements. However due to system calibration errors, the system may measure the Fourier transform at frequencies $\{u_i + \delta_i\}_{i=1}^M$ that are different from the base frequencies and where $\{\delta_i\}_{i=1}^M$ are unknown. Ignoring perturbations of this nature can lead to major errors in signal recovery. In this paper, we present a simple but effective alternating minimization algorithm to recover the perturbations in the frequencies *in situ* with the signal, which we assume is sparse or compressible in some known basis. In many practical cases, the perturbations $\{\delta_i\}_{i=1}^M$ can be expressed in terms of a small number of unique parameters $P \ll M$. We demonstrate that in such cases, the method leads to excellent quality results that are several times better than baseline algorithms.

Index Terms— Compressed sensing, Fourier measurements, Frequency Perturbations

1. INTRODUCTION

Compressed sensing (CS) is today a widely researched branch of signal processing. Consider a vector of compressive measurements $\boldsymbol{y} \in \mathbb{C}^M, \boldsymbol{y} = \boldsymbol{\Phi x}$ for signal $\boldsymbol{x} \in \mathbb{C}^N$, acquired through a sensing matrix $\boldsymbol{\Phi} \in \mathbb{C}^{M\times N}, M < N$. CS theory offers guarantees on the error of reconstruction of $\boldsymbol{x}$ that is sparse or compressible in a given orthonormal basis $\boldsymbol{\Psi} \in \mathbb{C}^{N\times N}$, assuming that the sensing matrix (also called measurement matrix) $\boldsymbol{\Phi} \in \mathbb{C}^{M\times N}$ (and hence the product matrix $\boldsymbol{\Phi\Psi}$) obeys some properties such as the restricted isometry (RIP) [1]. Moreover, the guarantees apply to efficient algorithms such as basis pursuit. However the underlying assumption is that the sensing matrix $\boldsymbol{\Phi}$ is known accurately. If $\boldsymbol{\Phi}$ is known inaccurately, then signal-dependent noise will be introduced causing substantial loss in reconstruction accuracy.

The email addresses of the authors are pandotra.himanshu@gmail.com, eeshan@gmail.com, ajitvr@cse.iitb.ac.in, karthik.gurumoorthy@icts.res.in.
AR acknowledges IITB seed grant #14IRCCSG012. KSG thanks the AIRBUS Group Corporate Foundation Chair in Mathematics of Complex Systems established in ICTS-TIFR.

Of particular interest in many imaging applications such as magnetic resonance imaging (MRI), tomography or Fourier optics [2, 3, 4, 5], is the case where the measurement matrix is a row-subsampled version of the Fourier matrix, where the frequencies may or may not lie on a Cartesian grid of frequencies used in defining the Discrete Fourier Transform (DFT). However, it is well-known that such Fourier measurements are prone to inaccuracies in the acquisition frequencies. This may be due to an imperfectly calibrated sensor. In case of specific applications such as MRI, this is due to perturbations introduced by gradient delays in the MRI machine [6, 7, 8]. In case of computed tomography (CT), it may be due to errors in specification of the projection angles due to geometric calibration errors in a CT machine [5], or in the problem of tomography under unknown angles [9]. The problem we deal within this paper is a special case of the problem of 'blind calibration' (also termed 'self-calibration') where perturbations in the sensing matrix are estimated *in situ* along with the signal. Here, we expressly deal with the case of Fourier sensing matrices with imperfectly known frequencies. There exists a decent-sized body of earlier literature on the general blind calibration problem (not applied to Fourier matrices) beginning with theoretical bounds derived in [10]. Further on, [11] analyze a structured perturbation model of the form $\boldsymbol{y} = (\boldsymbol{A} + \boldsymbol{B\Delta})\boldsymbol{x}$ where $\boldsymbol{x}, \boldsymbol{\Delta}$ are the unknown signal and diagonal matrix of perturbation values respectively, and $\boldsymbol{A}, \boldsymbol{B}$ are the fully known original sensing matrix and perturbation matrix respectively. The theory is then applied to 'direction of arrival' (DOA) estimation in signal processing. Further work in [12] uses the notion of group-sparsity to infer the signal $\boldsymbol{x}$ and the perturbations $\boldsymbol{\Delta}$ using a convex program based on a first order Taylor expansion of the parametric DOA matrix. A total least squares framework that also accounts for sparsity of the signal is explored in [13] for a perturbation model of the form $\boldsymbol{y}+\boldsymbol{e} = (\boldsymbol{A}+\boldsymbol{E})\boldsymbol{x}$ where $\boldsymbol{e}, \boldsymbol{E}$ are the additive errors in the measurement vector $\boldsymbol{y}$ and measurement matrix $\boldsymbol{A}$ respectively. In [14], [15], [16],[17], the following framework is considered: $\boldsymbol{y} = \boldsymbol{\Delta A x}$, where $\boldsymbol{\Delta}$ is a diagonal matrix containing the unknown sensor gains which may be complex, $\boldsymbol{x}$ is the unknown sparse signal, and $\boldsymbol{A}$ is the known sensing matrix. Both $\boldsymbol{x}$ and $\boldsymbol{\Delta}$ are recovered together via linear least squares in [14], via the lifting technique on a biconvex prob-

lem in [15], using a variety of convex optimization tools in [16], and in [17] using a non-convex method. The problem we deal within this paper cannot be framed as a single (per measurement) unknown phase or amplitude shift/gain unlike these techniques, and hence is considerably different. Related to (but still very different from) the aforementioned problem of a perturbed sensing matrix, is the problem of a perturbed or mismatched signal representation matrix $\mathbf{\Psi}$ which can also cause significant errors in compressive recovery [18]. Note that in [18, 19, 12, 20], the emphasis is on mismatch in the representation matrix $\mathbf{\Psi}$ and *not* in the sensing matrix $\mathbf{\Phi}$.

To the best of our knowledge, there is no previous work on the analysis of perturbations in a Fourier *measurement* matrix in a *compressive sensing* framework. Some attempts have been made to account for frequency specification errors in MRI, however, most of these require a separate off-line calibration step where the perturbations are measured. However in practice, the perturbations in frequencies may be common to only subsets of measurements (or even vary with each measurement), and need not be static. In cases where the correction is made alongside the recovery step, a large number of measurements may be required [21], as the signal reconstruction does not deal with a compressed sensing framework involving ℓ_q ($q \leq 1$) minimization.

In Section 2 we define the problem and present a recovery algorithm with convergence analysis. Numerical results are presented in Section 3 followed by a conclusion in Section 4. A more detailed version of this work can be accessed at [22].

2. PERTURBED FOURIER COMPRESSED SENSING

2.1. Problem Definition

Formally, let $\boldsymbol{F} \in \mathbb{C}^{M\times N}$ be a Fourier matrix using a known (possibly, but not necessarily on-grid) frequency set $\boldsymbol{u} \triangleq \{u_i\}_{i=1}^{M} \in \mathbb{R}^M$, $\boldsymbol{x} \in \mathbb{R}^N$ be a signal that is sparse (with at the most s non-zero values) or compressible, measured using a perturbed Fourier matrix $\boldsymbol{F(\delta)} \in \mathbb{C}^{M\times N}$. Here, $\boldsymbol{\delta_{M\times 1}}$ represents a perturbation vector such that the matrix $\boldsymbol{F(\delta)}$ has frequencies $\boldsymbol{u+\delta}$. In many realistic application scenarios, values in $\boldsymbol{\delta}$ can be expressed in terms of a small number of unique parameters $\boldsymbol{\beta} \triangleq \{\beta_k\}_{k=1}^{P}$ where $P \ll M$. We henceforth term these 'perturbation parameters' (PPs). We divide the measurements into subsets, where the frequency perturbations for each subset can be expressed fully in terms of a *single* perturbation parameter from $\boldsymbol{\beta}$ (besides the base frequency itself). We assume that $\forall k, 1 \leq k \leq P, |\beta_k| \leq r$, where $r > 0$ is known. Let the k^{th} unique value in $\boldsymbol{\beta}$ correspond to the PP for measurements in subset L_k, indexing into the measurement vector $\boldsymbol{y}$. Thus $\forall i \in L_k, \delta_i = h(\beta_k, u_i)$ where h is a known function of the perturbation parameter β_k and base frequency u_i. The exact form of h is dictated by the specific application.

For example, in CT, tomographic projections are acquired at different angles. The 1D Fourier Transform of each such projection is equal to the 2D Fourier Transform along a radial spoke at the same angle (as per the 'Fourier Slice Theorem'). Let us define set L_k to contain indices of all frequencies along the k^{th} radial spoke at some angle α_k. The perturbation values δ_i for all base frequencies u_i in L_k can be expressed in terms of a single parameter - the error β_k in specifying the angle. Here, for frequency $u_i = (u_i^{(1)}, u_i^{(2)})$, we would have $\delta_i = h(\beta_k, u_i) \triangleq (\rho_i(\cos(\alpha_k+\beta_k)-\cos\beta_k), \rho_i(\sin(\alpha_k+\beta_k)-\sin\alpha_k))$ where $\rho_i = \sqrt{(u_i^{(1)})^2 + (u_i^{(2)})^2}, u_i^{(1)} = \rho_i \cos\alpha_k, u_i^{(2)} = \rho_i \sin\alpha_k$. There also exist similar applications for the case of gradient delays in MRI (see Sections II and III of [22]).

We now consider the following measurement model: $\boldsymbol{y} = \boldsymbol{F}(\boldsymbol{\beta})\mathbf{\Psi}\boldsymbol{\theta} + \boldsymbol{\eta}$, where $\boldsymbol{\eta}$ is a signal-independent noise vector, $\boldsymbol{F}(\boldsymbol{\beta})$ is a Fourier measurement matrix at the set of unknown frequencies $\boldsymbol{u+\delta} \triangleq \{u_i + \delta_i\}_{i=1}^{M}$, with $\delta_i = h(\beta_k, u_i)$ defined in terms of the PP β_k, an element of $\boldsymbol{\beta}$. We assume full knowledge of the base frequencies $\{u_i\}_{i=1}^{M}$. The problem is to recover *both*, the sparse signal coefficients $\boldsymbol{\theta}$, and the unknown PPs $\boldsymbol{\beta}$. This is formalized as follows:

$$\mathsf{P1}: \min_{\hat{\boldsymbol{\theta}},\hat{\boldsymbol{\beta}}\in[-r,r]^P} J(\hat{\boldsymbol{\theta}},\hat{\boldsymbol{\beta}}) \triangleq \|\hat{\boldsymbol{\theta}}\|_1 + \lambda\|\boldsymbol{y} - \hat{\boldsymbol{F}}(\hat{\boldsymbol{\beta}})\mathbf{\Psi}\hat{\boldsymbol{\theta}}\|_2, \quad (1)$$

where $\boldsymbol{\theta} = \mathbf{\Psi}^T\boldsymbol{x}$ are the sparse/compressible coefficients of signal $\boldsymbol{x}$ in basis $\mathbf{\Psi}$. We emphasize that the problem P1 is *very different* from the problem of joint CS under motion (i.e., recovery of signal along with motion parameters) with Fourier measurement matrices. To see this, consider the case when the function $h(.)$ is identity, i.e. $\forall i \in \{1, ..., M\}, \delta_i = \beta_i$. In such a case, the forward model for the measurements can be written as $\boldsymbol{y} = \boldsymbol{FD}\mathbf{\Psi}\boldsymbol{\theta}$ where $\boldsymbol{D}$ is a $N \times N$ diagonal matrix such that $D_{kk} = \exp(-\iota 2\pi\delta_k l/N)$ where l, k are the spatial and measurement index respectively. For the CS under motion problem, the forward model would instead have the form: $\boldsymbol{y} = \tilde{\boldsymbol{D}}\boldsymbol{F}\mathbf{\Psi}\boldsymbol{\theta}$ where $\tilde{\boldsymbol{D}}$ is a $M \times M$ diagonal matrix such that $\tilde{D}_{kk} = \exp(-\iota 2\pi u_k\tilde{\delta_k}), k \in \{1, ..., M\}$ and $\tilde{\delta_k}$ is the translation of the signal in the k^{th} frame.

2.2. Recovery Algorithm

To solve P1, the following two sub-problems are considered.

- **Step I**: Given the current estimate of $\boldsymbol{\beta}$, solve for the best $\boldsymbol{\theta}$ as: $\text{argmin}_{\hat{\boldsymbol{\theta}}} \|\hat{\boldsymbol{\theta}}\|_1$ s.t. $\|\boldsymbol{y} - (\boldsymbol{F}(\boldsymbol{\beta})\mathbf{\Psi}\hat{\boldsymbol{\theta}})\|_2^2 \leq \varepsilon$.
- **Step II**: Given the current estimate of $\boldsymbol{\theta}$, solve for $\boldsymbol{\beta}$ as: $\boldsymbol{\beta} = \text{argmin}_{\hat{\boldsymbol{\beta}}} \|\boldsymbol{y} - \boldsymbol{F}(\boldsymbol{\beta})\mathbf{\Psi}\boldsymbol{\theta})\|_2^2$ s.t. $\forall k \in \{1, ..., P\}, |\beta_k| \leq r$.

The problem in Step I is solved via a standard basis pursuit denoising (BPDN) algorithm and the parameter ε is dependent on the noise variance. The problem in Step II is a highly non-convex problem. But it can be efficiently solved by *independent* brute-force search for each PP β_k in the form

$\text{argmin}_{\hat{\beta}_k, |\hat{\beta}_k| \leq r} \sum_{i \in L_k} \|y_{ik} - \boldsymbol{F}_i(\hat{\beta}_k)\boldsymbol{\Psi}\boldsymbol{\theta}\|_2^2$. The alternating minimization steps are performed iteratively till convergence.

2.3. Convergence

We prove convergence of Alg. 2.2 under a specific condition mentioned further. Let $\boldsymbol{F_\delta}$ denote the Fourier transform computed at the frequency values $\boldsymbol{u} + \boldsymbol{\delta}$ where $\boldsymbol{\delta} = h(\boldsymbol{\beta}, \boldsymbol{u})$. Assign $\boldsymbol{z} = \{\boldsymbol{x}, \boldsymbol{\beta}\}$. Recall that our objective is to determine the solution $\boldsymbol{z}^* = \text{argmin}_{\boldsymbol{z}} J(\boldsymbol{z})$ in Eqn. 1. Let $\boldsymbol{z_t} = \{\boldsymbol{x_t}, \boldsymbol{\beta_t}\}$ be the present solution of our alternating search algorithm at iteration t. Our alternating search algorithm ensures that the sequence of function values $\{J(\boldsymbol{z_t})\}_{t \in \mathbb{N}}$ is monotonically decreasing. As J is bounded below by 0, the sequence $\{J(\boldsymbol{z_t})\}_{t \in \mathbb{N}}$ converges to a limit value $E \in \mathbb{R}^+$ by the monotone convergence theorem. To prove the convergence of the solution sequence $\{\boldsymbol{z_t}\}$, let $\boldsymbol{x}(\boldsymbol{\beta})$ denote the minimizer for the convex objective function on $\boldsymbol{x}$ with $\boldsymbol{\beta}$ held fixed, namely $\boldsymbol{x}(\boldsymbol{\beta}) = \text{argmin}_{\boldsymbol{x}} J_{\boldsymbol{\beta}}(\boldsymbol{x})$, where $J_{\boldsymbol{\beta}}(\boldsymbol{x}) = J(\boldsymbol{z})$ with $\boldsymbol{\beta}$ held constant. In the context of our alternating search algorithm, we have $\boldsymbol{x}_{t+1} = \boldsymbol{x}(\boldsymbol{\beta}_t)$. Letting $\boldsymbol{z}_{t+\frac{1}{2}} = \{\boldsymbol{x}_{t+1}, \boldsymbol{\beta}_t\}$ we find that $\|\boldsymbol{x}_{t+1}\|_2 \leq \|\boldsymbol{x}_{t+1}\|_1 \leq J\left(\boldsymbol{z}_{t+\frac{1}{2}}\right) = J_{\boldsymbol{\beta}_t}(\boldsymbol{x}_{t+1}) \leq J_{\boldsymbol{\beta}_t}(\boldsymbol{0}) = \lambda\|\boldsymbol{y}\|_2$, giving an upper bound on the norm of $\boldsymbol{x}_t$. The last but one inequality follows from that fact that $\boldsymbol{x}_{t+1}$ minimizes $J_{\boldsymbol{\beta}_t}(\boldsymbol{x})$. Further, as $-r \leq \beta_i \leq r$ for each i, we see that the sequence $\{\boldsymbol{z}_t\}_{t \in \mathbb{N}}$ lie within a compact space. Hence as per Theorem 4.9 in [23], this sequence has at least one accumulation point. Another statement in the same theorem states that if a certain condition is satisfied, then $\lim_{t \to \infty} \|\boldsymbol{z}_{t+1} - \boldsymbol{z}_t\| = 0$, which establishes convergence of the solution. The condition is that for each such accumulation point, the minimization of $J(\boldsymbol{z})$ gives (i) a unique solution for $\boldsymbol{x}$ if $\boldsymbol{\beta}$ is fixed, and (ii) a unique solution for $\boldsymbol{\beta}$ if $\boldsymbol{x}$ is fixed. Condition (i) is easy to satisfy as the problem is convex in $\boldsymbol{x}$ if $\boldsymbol{\beta}$ is fixed. We do not have a theoretical proof for Condition (ii), but we have observed uniqueness experimentally, especially since the values in $\boldsymbol{\beta}$ are bounded between $-r$ to $+r$. As an example, in Fig. 1, we show a plot of the function $\|\boldsymbol{y} - \boldsymbol{F_\delta}\boldsymbol{x}\|^2$ keeping $\boldsymbol{x}$ and all but one value in $\boldsymbol{\delta}$ fixed. Note that here $\boldsymbol{x}$ denotes the estimated signal value upon (empirically observed) convergence of Alg. 2.2. We would like to emphasize that Theorem 4.9 in [23] only requires continuity of the function J and no other conditions like biconvexity. Given the non-convexity of J, global guarantees are very difficult to establish.

3. EXPERIMENTAL RESULTS

Recovery of 1-D signals: We present recovery results on 1D signals using Alg. 2.2 in Fig. 2. 1D signals of $N = 101$ elements were used. In Fig. 2, the signal sparsity $s \triangleq \|\boldsymbol{x}\|_0$ was varied along the x-axis, and the number of measurements M was varied along the y-axis. The cell at the intersection depicts the relative recovery error (RRMSE), $\frac{\|\boldsymbol{x} - \hat{\boldsymbol{x}}\|_2}{\|\boldsymbol{x}\|_2}$, averaged across 5 different signals. For any sparsity level, the signals were generated using randomly chosen supports with random values at each index in the support. The base frequencies $\boldsymbol{u}$ for the M Fourier compressive measurements for each signal were chosen uniformly randomly from $\{-N/2, -N/2 + 1, ..., N/2\}$. Each base frequency was subjected to perturbations chosen from Uniform$[-r, +r]$, with $r = 0.5$. For this experiment, we chose $P = 2$ unique values for the perturbations, i.e. $\forall i \in \{1, ..., M\}, \exists! k \in \{1, 2\}$ s. t. $\delta_i = \beta_k$. To the Fourier measurements thus simulated, noise from $\mathcal{N}(0, \sigma^2)$ was added, where $\sigma \triangleq 0.05\times$ average noiseless measurement magnitude. We compared our recovery algorithm to a baseline approach which ignores the perturbations and recovers the signal using a straightforward basis pursuit approach, with the *unperturbed, on-grid* Fourier matrix as the measurement matrix, i.e. assuming $\boldsymbol{\delta} = \boldsymbol{0}$. We term this approach the 'Baseline'. In Fig. 2, black (RGB (0,0,0)) indicates perfect recovery, and white (RGB (1,1,1)) indicates recovery error of 100% or higher. In all experiments, a multi-start strategy with 10 starts was adopted to combat the non-convexity of $J(\boldsymbol{\theta}, \boldsymbol{\beta})$, and the solution which yielded the least value of this objective function was selected. Note that the regularization parameter λ in Eqn. 1 was chosen by cross-validation on a small 'training set' of signals. The same λ was used in all experiments. From Fig 2, we observe that our results are easily superior to the Baseline.

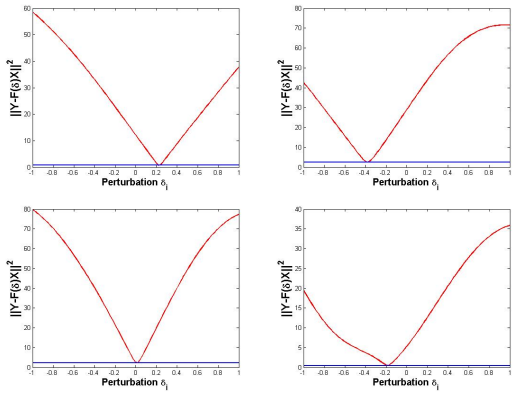

Fig. 1: Uniqueness of the solution for a single perturbation value δ keeping the estimated signal $\boldsymbol{x}$ (at empirically observed convergence of Alg. 2.2) fixed. Left to right, top bottom, for: (a) $M = 30, s = 10$, (b) $M = 50, s = 30$, (c) $M = 60, s = 30$, (d) $M = 20, s = 10$ where s is true signal sparsity

Recovery of 2-D signals: Application of Alg. 2.2 to 2D images more closely reflects practical imaging scenarios. We first present results with a similar set of toy experiments using 2D images (as the signal $\boldsymbol{x}$). For this experiment, 30×30 images were used. The images were generated using a sparse linear combination of Haar wavelet bases. We used a radial

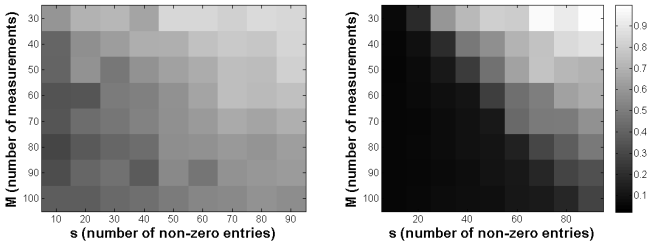

(a) (b)

Fig. 2: Recovery with Proposed Alternating Minimization algorithm for a 1D signal with 101 elements, sparse in canonical basis, 5% zero mean Gaussian noise added to measurements. (a) Baseline (b) Our Approach, with $r = 0.5$, $P = 2$ where P represents #unique perturbation parameter values.

sampling approach in the Fourier domain (equivalent to taking a Fourier transform of the Radon projections), taking a fixed number of measurements along each spoke, but varying the number of angles used and the sparsity of the image in the HWT basis. The angles for the spokes were incorrectly specified (which is typical in mis-calibrated tomography) with each angle error chosen from Uniform$[-2^\circ, +2^\circ]$ - leading to *significant* perturbations in the frequencies. The base frequencies $\boldsymbol{u}$ were spaced uniformly along each spoke. In addition, 5% zero mean i.i.d. Gaussian noise was added to the measurements (both real and complex parts, independently). We used the YALL1[1] solver for optimization of $\boldsymbol{x}$ and the NUFFT package[2] for computing Fourier transforms at non-integer frequencies. The results are summarized in a chart shown in Fig. 3. As Fig. 3 shows, the recovery error was small, even for a

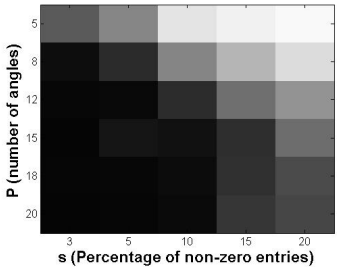

Fig. 3: Recovery error for 30×30 2D image, sparse in 2D Haar Wavelet basis, with 5% zero mean Gaussian measurement noise and angle errors from Uniform$[-2^\circ, +2^\circ]$

reasonably small number of measurements, and the method was robust to noise in the measurements. In the second set of experiments, we show reconstruction results on three images each of size 200×200. Fourier measurements were simulated along 140 radial spokes with erroneously specified angles (which is typical in tomography with angle errors or unknown angles). The angle error for each spoke was chosen independently from Uniform$[-3^\circ, +3^\circ]$ - leading to *significant* perturbations in the frequencies. Noise from $\mathcal{N}(0, \sigma^2)$ where $\sigma \triangleq 0.05\times$ average (noiseless) measurement magnitude, was added to the real and complex parts of the measurements. During reconstruction, we exploited image sparsity in a Haar wavelet basis. Reconstruction results with Alg. 2.2 are presented in Fig. 4. In comparison with the Baseline, we see that our algorithm performs significantly better in terms of RRMSE values as well as visually.

[1]http://yall1.blogs.rice.edu/

[2]https://www-user.tu-chemnitz.de/ potts/nfft/

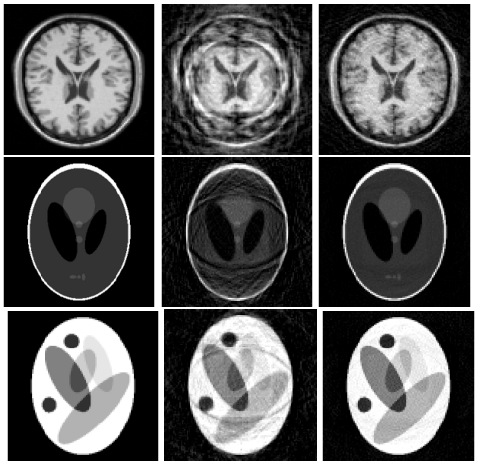

Fig. 4: Results for 200×200 images with 5% zero mean Gaussian measurement noise, 70% compressive measurements, angle error from Uniform$[-3^\circ, +3^\circ]$. In each row, left: original image, middle: result using Baseline (RRMSE $38.75\%, 35.48\%, 14.59\%$), right: result using Alg. 2.2 (RRMSE $13.15\%, 5.29\%, 5.85\%$). Zoom in pdf for details.

4. CONCLUSION

We have presented a simple, noise-robust, theoretically well-grounded method to correct for perturbations in a compressive Fourier sensing matrix *in situ* during signal reconstruction. We have discussed several applications of our framework, and have proved conditional convergence of Alg. 2.2. In Alg. 2.2 and its analysis, we have consciously avoided using a first order Taylor approximation, unlike the approaches for basis mismatch in [11, 12]. Even though Taylor approximation may appear to simplify (linearize) the problem, it introduces significant truncation errors. Our experimental results justify our choice to avoid this method (see section IV of [22]). Future work will involve proving analytical bounds for the global optimum of Alg. 2.2, which we believe will be stronger than those provided by results from standard CS [1], MMV [24] or GMMV [25] applied to this problem. We also aim to explore our algorithm in practical MRI/CT acquisition.

5. REFERENCES

[1] E. Candès and M. Wakin, "An introduction to compressive sampling," *IEEE signal processing magazine*, vol. 25, no. 2, pp. 21–30, 2008.

[2] O. Katz, J. Levitt, and Y. Silberberg, "Compressive fourier transform spectroscopy," 2010, Optical Society of America.

[3] P. Schniter and S. Rangan, "Compressive phase retrieval via generalized approximate message passing," *IEEE Trans. Signal Processing*, vol. 63, no. 4, pp. 1043–1055, 2015.

[4] M. Lustig, "Compressed sensing MRI," *IEEE Signal Processing Magazine*, 2008.

[5] M. Ferrucci, R. Leach, C. Giusca, S. Carmignato, and W. Dewulf, "Towards geometrical calibration of X-ray computed tomography systems: a review," *Measurement Science and Technology*, vol. 26, no. 9, pp. 092003, 2015.

[6] H. Jang and A. McMillan, "A rapid and robust gradient measurement technique using dynamic single-point imaging," *Magnetic Resonance in Medicine*, 2016.

[7] R. Robison, A. Devaraj, and J. Pipe, "Fast, simple gradient delay estimation for spiral MRI," *Magnetic resonance in medicine*, vol. 63, no. 6, pp. 1683–1690, 2010.

[8] E. Brodsky, A. Samsonov, and W. Block, "Characterizing and correcting gradient errors in non-cartesian imaging: Are gradient errors linear-time-invariant?," *Magnetic Resonance Imaging*, vol. 62, pp. 1466–1476, 2009.

[9] E. Malhotra and A. Rajwade, "Tomographic reconstruction from projections with unknown view angles exploiting moment-based relationships," in *ICIP*, 2016, pp. 1759–1763.

[10] M. Herman and T. Strohmer, "General deviants: An analysis of perturbations in compressed sensing," *J. Sel. Topics Signal Processing*, vol. 4, no. 2, pp. 342–349, 2010.

[11] Z. Yang, C. Zhang, and L. Xie, "Robustly stable signal recovery in compressed sensing with structured matrix perturbation," *IEEE Transactions on Signal Processing*, vol. 60, no. 9, pp. 4658–4671, 2012.

[12] T. Zhao, Y. Peng, and A. Nehorai, "Joint sparse recovery method for compressed sensing with structured dictionary mismatches," *IEEE Transactions on Signal Processing*, vol. 62, no. 19, pp. 4997–5008, 2014.

[13] H. Zhu, G. Leus, and G. Giannakis, "Sparsity-cognizant total least-squares for perturbed compressive sampling," *IEEE Transactions on Signal Processing*, vol. 59, 2011.

[14] S. Ling and T. Strohmer, "Self-calibration via linear least squares," *CoRR*, vol. abs/1611.04196, 2016.

[15] S. Ling and T. Strohmer, "Self-calibration and biconvex compressive sensing," *Inverse Problems*, vol. 31, 2015.

[16] C. Bilen, G. Puy, R. Gribonval, and L. Daudet, "Convex optimization approaches for blind sensor calibration using sparsity," *IEEE Transactions on Signal Processing*, vol. 62, no. 8, pp. 4847–4856, 2014.

[17] V. Cambareri and L. Jacques, "A non-convex blind calibration method for randomised sensing strategies," in *Intnl Workshop on Compressed Sensing Theory and its Applications to Radar, Sonar and Remote Sensing*, 2016, p. 16–20.

[18] Y. Chi, L. L. Scharf, A. Pezeshki, and R. Calderbank, "Sensitivity to basis mismatch in compressed sensing," *IEEE Trans. Signal Processing*, vol. 59, no. 5, pp. 2182–2195, 2011.

[19] G. Tang, B. N. Bhaskar, P. Shah, and B. Recht, "Compressed sensing off the grid," *IEEE Trans. Information Theory*, vol. 59, no. 11, pp. 7465–7490, 2013.

[20] J. Nichols, A. Oh, and R. Willett, "Reducing basis mismatch in harmonic signal recovery via alternating convex search," *IEEE Signal Process. Lett.*, vol. 21, no. 8, pp. 1007–1011, 2014.

[21] J. Ianni and W. Grissom, "Trajectory auto-corrected image reconstruction," *Magnetic resonance in medicine*, vol. 76, no. 3, pp. 757–768, 2016.

[22] E. Malhotra, H. Pandotra, A. Rajwade, and K. S. Gurumoorthy, "Signal recovery in perturbed fourier compressed sensing," `https://arxiv.org/abs/1708.01398`, 2017.

[23] J. Gorski, F. Pfeuffer, and K. Klamroth, "Biconvex sets and optimization with biconvex functions: a survey and extensions," *Mathematical Methods of Operations Research*, vol. 66, no. 3, pp. 373–407, Dec 2007.

[24] M. F. Duarte and Y. C. Eldar, "Structured compressed sensing: From theory to applications," *Trans. Sig. Proc.*, vol. 59, no. 9, pp. 4053–4085, 2011.

[25] R. Heckel and H. Bölcskei, "Joint sparsity with different measurement matrices," in *Allerton Conference on Communication, Control, and Computing*, 2012, pp. 698–702.